BOREAL ENVIRONMENT RESEARCH 14: 297–304
ISSN 1239-6095 (print) ISSN 1797-2469 (online)
© 2009
Helsinki 30 April 2009

Upwelling characteristics derived from satellite sea surface temperature data in the Gulf of Finland, Baltic Sea

Rivo Uiboupin and Jaan Laanemets

Marine Systems Institute at Tallinn University of Technology, Akadeemia tee 21, 12618 Tallinn, Estonia (e-mail: Rivo.Uiboupin@phys.sea.ee)

Received 9 May 2007, accepted 17 March 2008 (Editor in charge of this article: Timo Huttula)

Uiboupin, R. & Laanemets, J. 2009: Upwelling characteristics derived from satellite sea surface temperature data in the Gulf of Finland, Baltic Sea. *Boreal Env. Res.* 14: 297–304.

The seven-year (2000–2006) satellite sea surface temperature (SST) data were examined to determine characteristics of coastal upwellings during the warm period of the year (June–September) in the Gulf of Finland. A total of 20 sufficiently cloud-free SST images depicting well-expressed coastal upwelling were found. The area covered by upwelling water, the temperature difference between the upwelling and surrounding waters, and the location and area of filaments were estimated. The average area covered by the upwelling water was 4820 km^2 and for the largest upwelling event 12 140 km^2, i.e. 38% of the Gulf surface area. The average upwelling area along the Finnish coast (6120 km^2) was larger than the upwelling area along the Estonian coast (4070 km^2) which likely results from a larger cumulative wind stress (the product of wind stress and its duration) of westerly winds during the observed upwellings. The detected upwelling filaments were predominantly related to an upwelling along the Finnish coast. The area of a single filament usually varied from 80 to 680 km^2 while the total area of filaments reached the maximal value of 1420 km^2 during the strongest upwelling event.

Introduction

The coastal upwelling caused by the alongshore wind forcing typically brings cold and nutrient-rich deeper water to the surface layer. In the Gulf of Finland, summer upwellings usually transport cold and phosphate rich water from thermocline to the surface thus promoting the growth of nitrogen-fixing cyanobacteria (e.g. Haapala 1994, Vahtera *et al*. 2005). Besides the field measurements and numerical modeling the satellite sea surface temperature (SST) data carries substantial additional information about the spatial extent and structure of wind-driven coastal upwellings. Concerning the Baltic Sea, the satellite sea surface temperature images have been analysed by Horstmann (1983), Bychkova and Victorov (1986), Gidhagen (1987), Siegel *et al*. (1994) and Kahru *et al*. (1995) to determine upwelling parameters for the period with thermally stratified sea. They found that the temperature difference between the upwelled and surrounding water varies within 2–10 °C, the alongshore extent is of the order of hundreds kilometres and the off-shore scale is tens of kilometres.

The seasonal thermocline in the Gulf of Finland usually forms at the beginning of May, is at its strongest in July–August and erodes by the end of August (e.g. Alenius *et al*. 1998). Its

depth is of 10–15 m and in July–August the temperature difference between the warm surface layer and the cold intermediate layer below the thermocline may be up to 20 °C. Therefore, due to the strong thermal stratification the large sea surface temperature contrasts could be expected in the upwelling regions. Owing to the prevailing south-westerly winds (e.g. Mietus 1998, Soomere and Keevallik 2003) the northern coastal sea of the Gulf of Finland is an active upwelling area in summer as it was shown also by model simulations (Myrberg and Andrejev 2003). Kahru *et al*. (1995) identified from satellite SST images that the northwestern Gulf of Finland is one of the major upwelling front areas in the Baltic Sea. They found two most significant upwelling centres where filaments emerge from the upwelling front off the Hanko and Porkkala peninsulas and move south towards the Estonian coast. The model simulations showed also that the mesoscale disturbances (meanders and eddies) of an alongshore upwelling jet can be attributed to topographic irregularities (e.g. Zhurbas *et al*. 2004).

The objective of this work was to estimate the surface area covered by the upwelling water, the location of upwelling filaments and the temperature difference between the upwelling and surrounding water during summer upwelling events in the Gulf of Finland. The study is based on examination of satellite SST data from the years 2000–2006.

Data and methods

Remote sensing and wind data

The 7-year (2000–2006) SST data measured by MODerate Resolution Imaging Spectroradiometer (MODIS) onboard of Terra and Aqua satellites were used in this study. Both satellites overpass the Baltic Sea daily. MODIS Level 2 products, MOD28L2 and MYD28L2 provide sea surface temperature calculated from the long wavelength (11–12 μm) and the short wavelength (3–4 μm) bands at about 1×1 km resolution. Previous studies (Brown and Minnett 1999, Reinart and Reinhold 2008) have confirmed that the SST measurements can be considered having the accuracy of up to ±0.5 °C. The SST images from the warm period of the year (June–September) were analysed in the present study.

Wind data measured at the Kalbådagrund weather station (Fig. 1) (Finnish Meteorological Institute) were used for the calculation of the approximate along-gulf component of the cumulative wind stress (the product of the wind stress and its duration) to estimate the wind forcing during the observed upwelling events and to count the summer wind events favourable for upwelling. Soomere and Keevallik (2003) analysed wind data series from weather stations around the Gulf and found that the wind data measured at the southern coast do not represent adequately marine wind properties. Therefore we used Kalbådagrund weather station data for the calculation of both, easterly and westerly, wind forcing. The gaps in the Kalbådagrund wind data record (September 2000 and July 2003) were filled out with the wind data measured at the Utö weather station (Finnish Meteorological Institute).

Methods

In order to exclude the areas covered by clouds or influenced by coast, the reflectance data from MODIS bands 1 (620–670 nm) and 2 (841–876 nm) were examined together with MODIS SST data.

The line between the Hanko peninsula and the island of Osmussaar is treated as the western boundary of the Gulf of Finland basin (line A in Fig. 1). For detection of the border of the upwelling water (including filaments) the computer software ENVI 4.2 (ENVI 2001) was used. The SST images were overlaid by isotherms with the fixed contour interval of 0.5 °C starting from the upwelling centre(s). All sea surface isotherms either form closed contours or intersect the basin boundary. The contour of the warmest isotherm intersecting the basin boundaries is considered the upwelling water open sea border (Fig. 2a).

The pixels belonging to the upwelling water region were counted and also marked for visual checking of the upwelling water area. The total area of upwelling water was calculated from the known pixel area for each particular SST image.

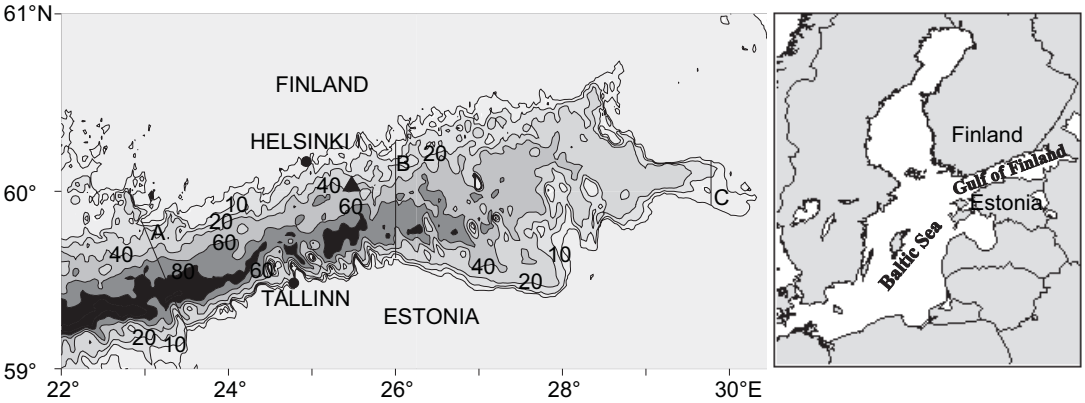

Fig. 1. The Baltic Sea (right panel) and the map of the Gulf of Finland (left panel) with the depth contours drawn from the gridded topography (Seifert *et al.* 2001). Shown is the location of Kalbådagrund (▲) weather station. The Gulf area is divided into two parts: western Gulf between lines A and B and eastern Gulf between lines B and C.

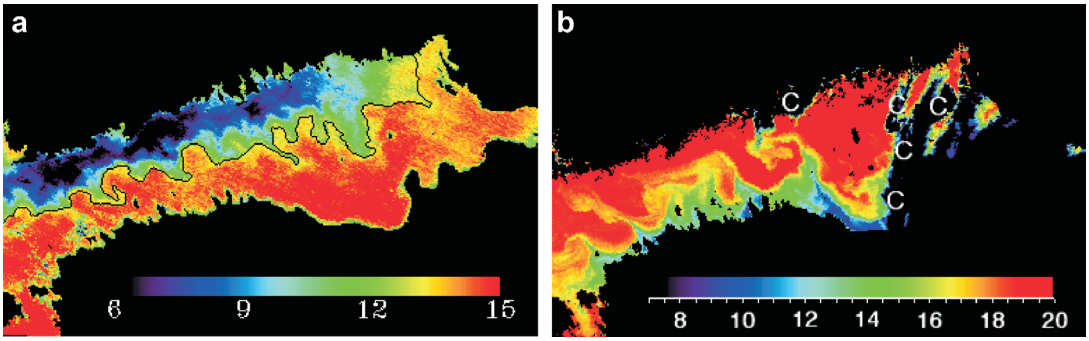

Fig. 2. — **a**: The largest upwelling observed during the study period on 24 September 2003 along the Finnish coast. The determined border of upwelling water is marked by a solid curve. — **b**: A large upwelling observed during the study period on 25 August 2006 along the Estonian coast. C = cloud cover.

The filament location was defined coinciding with the filament width centre along the edge of upwelling front. The filament length was defined as the distance from the filament location to the farthest filament pixel. The filaments with the length larger than the width and with the area larger than 50 km^2 were taken into account.

Results

Detected and potential upwelling events

We found 20 sufficiently clear sky SST images comprising five upwelling events along the Finnish coast and five events along the Estonian coast during the summers 2000–2006. The wind data records from June to the end of September (2000–2005) showed yearly five to eight (on the average about six per year) upwelling-favourable wind events per summer which had the absolute along-gulf component of the cumulative wind stress larger than 0.1 N m^{-2} d. The frequency of wind events able to generate upwelling were different along the Estonian and Finnish coast and varied considerably from year to year. We found one to four (on the average about two) wind events (June–September) that might generate upwellings along the Estonian coast and three to five (on the average about four) wind events that might generate upwellings along the Finnish coast for the study period. The westerly winds, caused by cyclones passing the Gulf area, are often accompanied by cloudy weather and, therefore, the fraction of SST images reflecting the upwelling events along the Finnish coast from all wind-detected upwelling-favorable events is smaller as compared with those from the similar

upwelling events along the Estonian coast, usually caused by anticyclones. Thus, taking into account the above statistics we observed about 20% from the potential upwelling events along the Finnish coast and about 40% along the Estonian coast during the study period.

Area covered with upwelling water

Calculations of the area covered by the upwelling water and its percentage were performed separately for the eastern and western parts of the Gulf of Finland considering the shape of the Estonian coastline (Fig. 1). On several occasions when clouds were partly covering either the Finnish or the Estonian coastal sea the percentages were calculated for the cloud free cross-Gulf stripe.

The average area covered by the upwelling water was 4820 km^2 which is about 15% from the total Gulf area. The average upwelling areas were larger along the Finnish coast (6120 km^2 and 19%) than along the Estonian coast (4070 km^2 and 13%). The most intensive upwelling along the Finnish coast occurred on 24 September 2003 (Fig. 2) and along the Estonian coast on 9 August 2006 when 38% (12 140 km^2) and 20% (6480 km^2) of the Gulf area respectively was covered with the upwelling water (Table 1).

Upwellings were more extensive in the western part of the Gulf, where the average area covered by the upwelling water was 3100 km^2 (22%) compared with 2420 km^2 (13%) in the eastern part. The average upwelling water areas along the Finnish and the Estonian coast were 3680 km^2 (26%) and 2630 km^2 (19%) in the western part of the Gulf. The corresponding esti-

Table 1. Upwelling characteristics in the western (WG) and eastern (EG) parts of the Gulf of Finland. The fraction of the cloudless area is presented in brackets in percents, the area covered with the upwelled water and the corresponding fraction in percents, the area of filaments, the minimum temperature (T_{min}) in the upwelling region, the maximum temperature (T_{max}) of the surrounding water across the front, their difference (ΔT) and the absolute along-gulf component of cumulative wind stress *W*. The areas of eastern and western part of the Gulf were about 18 000 km^2 and 14 000 km^2 correspondingly.

Coast	Date	Part of Gulf	Upwelling area (km^2)	Upwelling area (%)	Filament area (km^2)	T_{min} (°C)	T_{max} (°C)	ΔT (°C)	W N m^{-2}d
FIN	27 Sep. 2000	WG/EG	3047/2095	22/12	1020	14.4	17.9	3.5	0.52[a]
FIN	20 Jun. 2002	WG/EG	2917/1227	21/7	160	10.1	16.0	5.9	0.33
FIN	2 Sep. 2002	WG (32)	1808	40*	200	14.3	20.4	6.1	0.47
FIN	4 Sep. 2002	WG(60)/EG	2308/3921	28*/22	600	12.6	19.8	7.2	0.9
EST	17 Jul. 2003	WG/EG	1260/1121	9/6	–	10.7	21.3	10.6	0.21[b]
EST	19 Jul. 2003	WG/EG	2264/1923	16/11	230	10.1	20.5	10.4	0.23[b]
EST	21 Jul. 2003	EG(42)	783	10*	–	14.9	24.1	9.2	0.21[b]
EST	22 Jul. 2003	WG/EG	3598/2696	25/15	510	14.6	23.1	8.5	0.19[b]
EST	1 Aug. 2003	WG(36)/EG	249/1754	5*/10	–	11.0	25.1	14.2	0.06
EST	2 Aug. 2003	WG/EG	674/2297	5/13	110	10.3	25.5	15.2	0.06
FIN	23 Sep. 2003	WG(44)/EG	796/4951	13*/27	1170	7.7	14.8	7.1	1.52
FIN	24 Sep. 2003	WG/EG	6474/5664	46/31	1420	6.4	14.3	7.9	1.69
EST	9 Jul. 2005	WG(48)	990	14*	–	12.4	20.3	7.9	0.08
FIN	24 Sep. 2005	WG/EG(28)	4383/1108	31/22*	1330	7.9	15.2	7.4	0.98
FIN	25 Sep. 2005	WG	4336	31	1100	8.1	15.2	7.1	1.02
FIN	26 Sep. 2005	WG	3598	26	320	7.5	14.9	7.4	1.06
EST	6 Aug. 2006	WG/EG	2721/1406	19/8	–	7.2	20.1	12.9	0.51
EST	7 Aug. 2006	WG/EG	3666/2385	26/13	180	8.3	19.5	11.2	0.55
EST	9 Aug. 2006	WG/EG	4449/2031	31/11	160	7.2	18.0	10.8	0.59
EST	25 Aug. 2006	WG/EG(41)	4003/1734	29/24*	1400	8.7	19.2	10.5	0.47

* The area was partly covered by clouds; the percentage of area covered by upwelled water was calculated for cloudless area.

[a] Utö wind data.

[b] Combined wind data from Kalbådagrund and Utö.

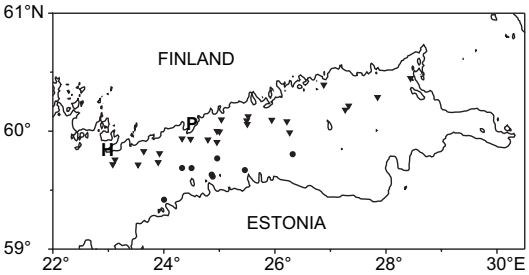

Fig. 3. Locations of upwelling filaments related to upwellings along the Finnish (▼) and Estonian (●) coast. Hanko and Porkkala peninsulas are marked with (H) and (P) correspondingly.

mates for the eastern part of the Gulf were 3440 km^2 (19%) and 1890 km^2 (10%).

Observed temperature differences between the upwelling and the surrounding water varied in a wide range, from 3.5 to 15.2 °C (Table 1). For the upwelling events along the Estonian coast the temperature differences were between 7.9 and 15.2 °C. During upwelling events along the Finnish coast the temperature differences were smaller, from 3.5 to 7.9 °C.

Upwelling filaments

Overall 32 filaments, excluding the filaments of coinciding location observed on the successive SST images of the same upwelling event, were identified. The filaments predominantly stretched out from the upwelling front along the Finnish coast and in the western part of the Gulf (Fig. 3). Only eight filaments were related to the upwellings along the Estonian cost thereby 6 of those were observed during the strongest upwelling event along the Estonian coast in August 2006.

The length of filaments was up to 35 km and in several cases the filaments observed along the northern coast were cyclonically turned. For example, on the SST images from 24 to 26 September 2005 the cyclonically turned filaments can be detected along the Finnish coast (Fig. 4a) which further on formed a rotating vortex pair and an eddy (Fig. 4b and c). The area of single filaments varied in a wide range from 80 to 680 km^2.

The area covered by filaments was significantly larger for the upwellings along the northern coast as the filaments were rarely formed

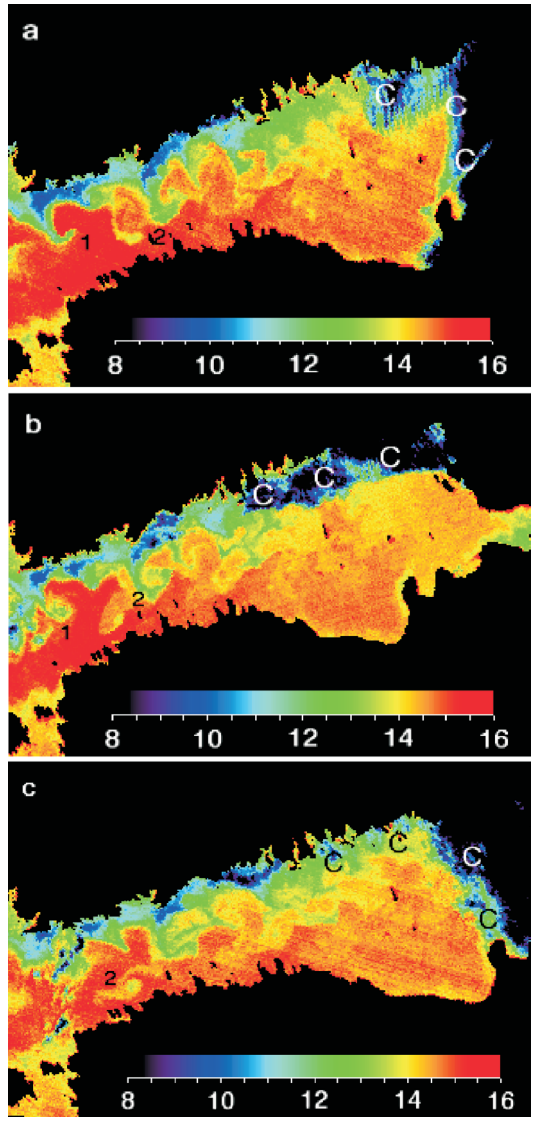

Fig. 4. Series of SST images showing the development of filaments emerging from the upwelling front along the Finnish coast during 24–26 September 2005. Filament marked as 1 in panel **a** turned into eddy (*see* **b**). Filament marked as 2 in panel **a** formed a rotating vortex pair (*see* **b**), one of which turned into eddy (*see* **c**). C = cloud cover.

in case of upwellings along the southern coast (Table 1). In case of the largest upwelling event along the Finnish coast observed on 24 September 2003 (Fig. 2a) the area of filaments was 1420 km^2 (Table 1) which made up 12% from the total area of the upwelled water in the Gulf. The share of upwelling filaments was higher in the western part of Gulf. For example, during the upwelling

along the Finnish coast on 24 September 2005 (Fig. 4a) the area of filaments was 1330 km^2 (30%) and during a large upwelling along the Estonian coast on 25 August 2006 (Fig. 2b) the area of filaments was 1100 km^2 (27%).

Discussion and conclusions

Satellite SST images allow upwelling characteristics study all over the entire area of the Gulf. The summer upwellings in the Gulf of Finland are characterized by pronounced temperature contrasts which provide a good premise for identification of upwelling events and their parameters from SST images. Due to the high cloudiness level the weakness of the Baltic Sea satellite SST data are a relatively small fraction (10%–50%) of useful images suitable for processing (e.g. Krężel *et al*. 2005).

Upwelling areas off the Finnish coast, on the average 6120 km^2, were larger as compared with those off the Estonian coast, 4070 km^2. During the strongest upwelling events observed on 24 September 2003 along the Finnish and on 9 August 2006 along the Estonian coast the upwelling water (including filaments) may cover remarkable areas, up to ~40 % and ~20% correspondingly from the total Gulf area (Table 1).

Considerably larger upwelling areas along the Finnish coastline could be explained by a larger westerly along-gulf component of cumulative wind stress that generated the observed upwelling events (Table 1). The cumulative wind stress was calculated from the beginning of the action of upwelling-favourable wind until the time of the satellite overpass. The approximate offshore displacement (ΔX) of the upwelling front is $\Delta X = W/\varrho_0 f h_E$, where W is the along-gulf component of cumulative wind stress, ϱ_0 is the reference density and h_E is the surface Ekman layer depth (Austin and Lentz 2002). This equation does not take into account the upwelling set-up time and there is also no data to estimate the Ekman layer depth. Nevertheless, the observed larger upwelling water areas along the Finnish coast were in accordance with larger cumulative wind stresses (Table 1).

The SST images from the study period showed that the pronounced cold filaments were related mainly to the upwelling events along the Finnish coast as it was also shown in an earlier study by Kahru *et al*. (1995). Although they found that filaments occurred mainly off Hanko and Porkkala peninsulas there were no easily seen preferred filament generation regions along the northern coast of the Gulf in our study (Fig. 3). The filaments originating from the coast of Estonia were weaker and were observed more rarely. The relatively high portion of upwelling water in the filaments, up to 30% in the western part of Gulf, points to their important role in the offshore transport of the cold and nutrient-rich water.

The generation of filaments is related to the instability of longshore baroclinic jet associated with the upwelling. Blumsack and Gierasch (1972) and de Szoeke (1975) showed that in case of sloping bottom the baroclinic instability of a longshore upwelling jet strongly depends on the ratio of the bottom slope to the isopycnal slope, α. When the isopycnal slope is smaller than the bottom slope ($\alpha > 1$) then the baroclinic instability of the upwelling jet is not expected to occur. A numerical study by Zhurbas *et al*. (2006) using the characteristic summer stratification in the Baltic Sea, also showed that no baroclinic instability of an upwelling jet was observed when the bottom slope exceeded the isopycnal slope. The cross-shore scale for the region of sloping isopycnals for the upwelling event is the baroclinic Rossby radius of deformation (Allen 1980). According to Fennel *et al*. (1991) the baroclinic Rossby radius of deformation is about 3 km in the Gulf of Finland in summer and the upper mixed layer depth is approximately 10 m, which gives a rough estimate for the isopycnal slope of 0.003. Although the bottom topography of the Gulf of Finland is complicated (Fig. 1) the approximate estimates of the bottom slope off the Estonian coast 0.006 and off the Finnish coast 0.002 could be used. Thus, in the Finnish coastal sea $\alpha \approx 0.5$ while in the Estonian coastal sea $\alpha > 1$, i.e. the baroclinic instability of the upwelling jet along the Finnish coast is more probable. Another reason of the observed difference between the occurrence of upwelling filaments along the Finnish and Estonian coasts is likely due to the different atmospheric forcing. The along-gulf component of cumulative wind stress was smaller during

the upwellings along the Estonian coast, except the upwelling on 25 August 2006 (Table 1). Zhurbas *et al*. (2006) showed that the instability growth rate depends on the cumulative wind stress and increases considerably for sufficiently large cumulative wind stresses.

Many filaments were cyclonically turned. The model simulations by Zhurbas *et al*. (2006) demonstrated the growth of wave-like perturbations forming mostly cyclonic meanders (filaments) of the upwelling jet which further on detached from the jet and formed mesoscale cyclonic eddies. Such development was also observed on a series of SST images (Fig. 4) with the time scale of a few days.

The detected upwellings off the Estonian coast occurred in July–August when the surface heating was strong and therefore the temperature difference between the upwelling and the surrounding waters was large while upwellings along the Finnish coast occurred in June and September and therefore the temperature difference was lower (Table 1).

To conclude, the analysis of satellite SST data showed that the upwelling water covered considerable area of the Gulf. Most likely due to the different atmospheric forcing and different topography of the northern and southern coasts of the Gulf the upwelling characteristics differed in the following way: (1) the upwellings off the northern coast were more extensive and the upwelling water covered larger areas of the coastal sea, and (2) the upwelling filaments were predominantly observed off the northern coast.

Acknowledgements: The Kalbådagrund and Utö weather station wind data were kindly provided by the Finnish Meteorological Institute. The temperature data on the transect Helsinki–Tallinn were kindly provided by Alg@line project (Estonian Marine Institute). Likewise, our thanks to Juss Pavelson, Aleksander Toompuu and Liis Sipelgas for valuable comments on the manuscript. This work was supported by Estonian Science Foundation through grant No. 7467.

References

Allen J.S. 1980. Models of wind driven currents on the continental shelf. *Annu. Rev. Fluid Mech*. 12: 389–433.

Alenius P., Myrberg K. & Nekrasov A. 1998. The physical oceanography of the Gulf of Finland: a review. *Boreal Env. Res*. 3: 97–125

Austin J.A. & Lentz S.J. 2002. The inner shelf response to wind-driven upwelling and downwelling. *J. Phys. Oceanogr*. 32: 2171–2193

Blumsack S.L. & Gierasch P.J. 1972. Mars: the effects of topography on baroclinic instability. *J. Atmos. Sci*. 29: 1081–1089.

Brown O.B. & Minnett P.J. 1999. *MODIS infrared sea surface temperature algorithm theoretical basis document*, ver. 2.0. Available at http://modis.gsfc.nasa.gov/data/atbd/atbd_mod25.pdf.

Bychkova I. & Viktorov S. 1986. Use of satellite data for identification and classification of upwelling in the Baltic Sea. *Oceanology* 27: 158–162.

de Szoeke R.A. 1975. Some effects of bottom topography on baroclinic instability. *J. Mar. Res*. 33: 93–122

Fennel W., Seifert T. & Kayser B. 1991. Rossby radii and phase speed in the Baltic Sea. *Cont. Shelf Res*. 11: 23–36.

ENVI 2001. *ENVI user's guide*. Research Systems Inc. Boulder CO.

Gidhagen L. 1987. Coastal upwelling in the Baltic — satellite and in situ measurements of sea surface temperatures indicating coastal upwelling. *Est. Coast. Shelf Sci*. 24: 449–462.

Haapala J. 1994. Upwelling and its influence on nutrient concentration in the coastal area of the Hanko Peninsula, entrance of the Gulf of Finland. *Est. Coast. Shelf Sci*. 38: 507–521.

Horstmann U. 1983. Distribution patterns of temperature and water colour in the Baltic Sea as recorded in satellite images: indicators for phytoplankton growth. *Bericthe aus dem Institute für Meereskunde an der Universität Kiel* 106: 1–147.

Kahru M., Håkansson B. & Rud O. 1995. Distributions of the sea-surface temperature fronts in the Baltic Sea as derived from satellite imagery. *Cont. Shelf Res*. 15: 663–679.

Krężel A., Ostrowski M. & Szymelfenig M. 2005. Sea surface temperature distribution during upwelling along the Polish Baltic coast. *Oceanologia* 47: 415-432.

Mietus M. 1998. *The climate of the Baltic Sea basin. Marine meteorology and related oceanographic activities*. Report 41, WMO/TD 933, Geneva.

Myrberg K. & Andrejev O. 2003. Main upwelling regions in the Baltic Sea — a statistical analysis based on three-dimentional modelling. *Boreal Env. Res*. 8: 97–112.

Reinart A. & Reinhold M. 2008. Mapping surface temperature in large lakes with MODIS data. *Rem. Sen. Env*. 112: 603–611.

Seifert T., Tauber F. & Kayser B. 2001. A high resolution spherical grid topography of the Baltic Sea, revised edition. In: *Baltic Sea Science Congress 2001: Past, Present and Future — A Joint Venture*, Abstract Volume, Stockholm University, pp. 298.

Siegel H., Gerth M., Rudolff R. & Tschersich G. 1994. Dynamic features in the western Baltic Sea investigated using NOAA-AVHRR data. *Dt. hydrogr. Z*. 46: 191–209.

Soomere T. & Keevallik S. 2003. Directional and extreme wind properties in the Gulf of Finland. *Proc. Estonian*

Acad. Sci. Eng. 9: 73–90.

Vahtera E., Laanemets J., Pavelson, J., Huttunen M. & Kononen K. 2005. Effect of upwelling on the pelagic environment and bloom-forming cyanobacteria in the western Gulf of Finland. Baltic Sea. *J. Mar. Syst.* 58: 67–82.

Zhurbas V.M., Stipa T., Mälkki P., Paka V.T., Kuzmina N.P. & Sklyarov V.E. 2004. Mesoscale variability of upwelling in the southeast Baltic: infrared images and numerical modeling. *Oceanology* 44: 495–504.

Zhurbas V.M., Oh I.S. & Park T. 2006. Formation and decay of a longshore baroclinic jet associated with transient coastal upwelling and downwelling: a numerical study with application to the Baltic Sea. *J. Geophys. Res.* 111(C4), C04014, doi: 10.1029/2005JC003079.